Colloids and Surfaces B: Biointerfaces 178 (2019) 74–79

Contents lists available at ScienceDirect

Colloids and Surfaces B: Biointerfaces

journal homepage: www.elsevier.com/locate/colsurfb

One-step synthesis of cellooligomer-conjugated gold nanoparticles in a water-in-oil emulsion system and their application in biological sensing

Mayumi Hatakeyama, Daisuke Ryuno, Shingo Yokota, Hirofumi Ichinose, Takuya Kitaoka[1,*]

Department of Agro-Environmental Sciences, Graduate School of Bioresource and Bioenvironmental Sciences, Kyushu University, 744 Motooka, Nishi-ku, Fukuoka, 819-0395, Japan

ARTICLE INFO

Keywords:
Cellooligomer
Gold nanoparticle
Lectin
N-methylmorpholine
N-oxide
Reverse micelle

ABSTRACT

Monodisperse gold nanoparticles (GNPs) were synthesized in a water-in-oil emulsion system (reverse micelles) composed of 80% *N*-methylmorpholine *N*-oxide (NMMO)/20% H_2O and dodecane, stabilized with an anionic surfactant: bis(2-ethylhexyl)sulfosuccinate sodium salt. Cellooligomers with a degree of polymerization of 6 or 15 (βGlc6 or βGlc15, respectively), which were labeled at each reducing end group with thiosemicarbazide (TSC) and dissolved in the aqueous NMMO phase, were successfully conjugated to the surfaces of GNPs *in situ* during spontaneous NMMO-mediated gold reduction. As-synthesized βGlc6-GNPs and βGlc15-GNPs had average diameters of 11.3 ± 2.1 and 10.5 ± 0.7 nm, respectively, while their surface sugar densities were 0.21 and 0.51 chains nm^{-2}, respectively. Concanavalin A (ConA), a lectin that recognizes non-reducing end groups of glucose residues, aggregated with βGlc15-GNPs with higher sensitivity than it did with βGlc6-GNPs, possibly as a result of the sugar density on the GNP surfaces. The aggregates were rapidly re-suspended by adding methyl-β-D-glucopyranoside as a binding inhibitor. Other lectins and proteins showed no interaction with βGlc-GNPs. Therefore, clustering of glucose non-reducing ends on the GNP surfaces *via* strong intermolecular association of cellooligomers, possibly led to high affinity for ConA. This facile synthesis route to structural carbohydrate-decorated GNPs has potential applications in carbohydrate–nanometal conjugate nano-biosensor development.

1. Introduction

Gold nanoparticles (GNPs) have recently attracted increasing attention owing to their unique properties arising from size-dependent electronic, magnetic, and optical properties (quantum size effects) [1,2], which make them relevant for bio-medical applications [3,4]. In particular, the characteristic surface plasmon resonance (SPR) of GNPs shows a sensitive dependence on their size at a nanometer level, resulting in an immediate color change from vivid red to deep purple with increasing particle size [1–7]. Such stimuli-responsive properties are required for high-performance sensing devices. Gold was chosen as it is very stable and bio-inert; in addition, GNP surfaces readily undergo spontaneous reactions with sulfur, amine, and carboxy moieties [8–10]. Thus, the bio-sensing applications of GNPs conjugated with biomolecules such as carbohydrates, nucleic acids, and peptides, which play significant roles in all living systems, have aroused significant interest in bio-active nanomaterial development [11–13].

Among the various substances used for the surface modification of GNPs, carbohydrates have attracted particular attention owing to their specific molecular characteristics and functions in various living systems, which result from their mutual interactions with proteins and cells [14,15]. Most biological processes are regulated by sugar-mediated noncovalent bonds, *i.e.* hydrogen bonds [16]. A diverse array of carbohydrates such as glucose (Glc), mannose (Man), galactose (Gal), *N*-acetylglucosamine (GlcNAc), and their oligomers/hybrids, which act as bio-active sugars *in vivo*, have been employed for conjugation with GNPs [17–21]. Uzawa et al. [22] reported that Gal-conjugated GNPs could detect toxalbumin ricin with high sensitivity through Gal-mediated binding. Duncan et al. [23] achieved the colorimetric detection of concanavalin A (ConA) using Man-conjugated GNPs, based on the specific interaction between Man and ConA. However, there are few reports that directly correlate the measured sugar density on GNP surfaces with such bio-interactions. Carbohydrate ligands *in vivo* assemble and reinforce their interactions with corresponding receptors, this is known as the cluster glycoside effect [24]. For example, carbohydrate-binding proteins, *i.e.* lectins, demonstrate a strong binding affinity for multivalent sugars several orders of magnitude greater than for single (monovalent) sugar ligands [25]. Therefore, tailoring of the

* Corresponding author.
E-mail address: tkitaoka@agr.kyushu-u.ac.jp (T. Kitaoka).
[1] http://bm.wood.agr.kyushu-u.ac.jp/index-e.html.

https://doi.org/10.1016/j.colsurfb.2019.02.051
Received 9 November 2018; Received in revised form 1 February 2019; Accepted 26 February 2019
Available online 27 February 2019
0927-7765/

surface sugar density is a key factor in the functional design of carbohydrate-conjugated GNPs. Chien et al. [26] reported that globotriose-conjugated GNPs demonstrated a different affinity for the subunit of Shiga toxin depending on the concentration ratios of conjugated sugars and GNPs; however the actual sugar density on the GNP surfaces remained unclear because of the difference in the conjugation efficiency of the as-designed globotriose moieties for GNPs. Thus, in most cases, the clustering effect of carbohydrates was insufficiently associated with the interaction between sugar-conjugated GNPs and targeted proteins.

Cellulose, a β-1,4-linked D-glucopyranose polymer, is the most typical structural polysaccharide and is the major constituent of plant cell walls [27]. Cellulose consists of water-soluble D-Glc only; however it dissolves in neither water nor organic solvents when its degree of polymerization (DP) is 7 or greater, owing to strong self-assembly through the formation of regular intra- and inter-molecular hydrogen bonds [28]. Such molecular features lead to a potential for amassing functional carbohydrate moieties, giving a cluster glycoside-like effect, on GNP surfaces; however conjugating cellulose with GNPs presents a significant challenge as there are no suitable solvents for both. In our previous study, the auto-redox synthesis of GNPs was achieved in an 80% *N*-methylmorpholine *N*-oxide (NMMO)/20% H_2O system [29]: a good solvent for various structural carbohydrates including cellulose. In addition, cellulose chains with DP 7 (βGlc7), 15 (βGlc15), and 200, which were labeled at their respective reducing end groups with thiosemicarbazide (TSC), were successfully conjugated to GNP surfaces *in situ* during GNP synthesis in the NMMO system. As-prepared cellulose-GNPs demonstrated unique self-assembling behavior; however they showed a broad size distribution due to the uncontrolled synthesis process, resulting in uncertain sugar density on each GNP surface.

In this study, a water-in-oil (W/O) emulsion consisting of 80% NMMO/20% H_2O and dodecane as the water and oil phases, respectively, which was stabilized with an anionic surfactant: sodium bis(2-ethylhexyl)sulfosuccinate (Aerosol-OT; AOT), was designed as an appropriate reaction medium for precise GNP synthesis and simultaneous glyco-conjugation using TSC-labeled βGlc6 and βGlc15 (βGlc6-TSC and βGlc15-TSC, respectively). It is thought that the limited volume of the W/O emulsion particles provided suitable conditions for the formation of monodisperse βGlc***n***-GNPs (***n*** = 6, 15). The size distribution of GNPs and the surface sugar density were investigated to estimate the Glc-clustering on the GNP surfaces. A carbohydrate-binding assay with ConA lectin from *Canavalia ensiformis* was carried out to evaluate the bio-sensing potential of βGlc-GNPs, and the cluster glycoside effect is discussed with regard to the affinity for ConA.

2. Experimental

2.1. Materials

Cotton cellulose powder (CF1, DP: *ca.* 200) was purchased from Whatman, UK. Water-insoluble cellooligomer with average DP values of 15 (βGlc15) were prepared from CF1 powder by phosphoric acid hydrolysis [30]. Water-soluble cellohexaose (βGlc6) was obtained from Seikagaku Corp. Japan. *N*-Methylmorpholine-*N*-oxide (NMMO) and tetrachloroauric acid ($HAuCl_4$) were obtained from Sigma-Aldrich. Thiosemicarbazide (TSC) and ConA were purchased from Wako, Japan. Aerosol-OT was obtained from Tokyo Chemical Industry. Peanut agglutinin (PNA) was purchased from J-OIL MILLS, Japan. Bovine serum albumin (BSA) was obtained from Merck Chemicals. The water used in this study was purified using a Milli-Q system (Millipore, USA). Other chemicals were reagent grade and used without further purification.

2.2. TSC-modification and synthesis of cellulose–GNP conjugates

βGlc***n*** samples (***n*** = 6, 15) were dissolved in 80 wt% NMMO/H_2O solution at 100 °C with stirring (concentration: 2 wt%), followed by aldehyde-selective thio-labeling by sequential addition of a molar equivalent of TSC, and heating at 65 °C for 90 min. The βGlc***n***-TSC derivatives were precipitated with ethanol, purified by repeated centrifugation (at least five times) to ensure complete removal of unreacted TSC molecules; then freeze-dried for storage.

GNPs were prepared by NMMO-mediated reduction of gold ions in a water-in-dodecane emulsion system stabilized with AOT. First, 0.089 g (0.2 mmol) of AOT in 2 mL of dodecane and 20 μL of 80% NMMO/20% H_2O (wt/wt) were mixed, and the micellar suspension was stirred at 70 °C for 15 min in an oil bath to maintain the temperature. Next, $HAuCl_4/H_2O$ (60 mmol L^{-1}, 20 μL) was added dropwise to the cloudy-white micro-emulsion under vigorous stirring and the emulsion immediately turned red.

In a similar manner, cellulose-conjugated GNPs were prepared using the one-step GNP synthesis and simultaneous *in situ* glyco-surface modification in NMMO/H_2O solvent [29] as a reverse micelle system. βGlc***n***-TSCs were dissolved in 80 wt% NMMO/H_2O solution at 100 °C for 30 min with stirring (βGlc***n*** concentration: 1.0, 2.0, 4.0, and 8.0 mmol L^{-1}) and added to the AOT/dodecane solution. Subsequently, an aqueous $HAuCl_4$ solution (60 mmol L^{-1}, 20 μL) was added dropwise to each microemulsion (total volume: *ca.* 2 mL) at 70 °C for 15 min with stirring. The emulsion also turned red immediately. An outline of the preparation procedures is summarized in Fig. 1.

2.3. Characterization

UV–vis spectra of carbohydrate-free and carbohydrate-conjugated GNPs were recorded at room temperature using a U-3000 spectrophotometer (Hitachi, Japan). Transmission electron microscopy (TEM) observation was carried out using a JEM1010 microscope (JEOL, Japan) at an accelerating voltage of 80 kV. For TEM and elemental analysis, as-synthesized GNPs samples were precipitated with methanol and purified by repeated centrifugation (at least three times) to completely remove NMMO and AOT; the precipitates were then freeze-dried. The simple precipitation with methanol also removed unreacted βGlc***n***-TSCs. In the case of βGlc15-GNPs, additional washing with 1 M NaOH solution that completely dissolves βGlc15-TSCs at room temperature was carried out to purify the βGlc15-GNPs through complete removal of unreacted βGlc15-TSCs. Deep purple-red powders of carbohydrate-free and carbohydrate-conjugated GNPs were suspended in deionized water, and mounted on carbon-coated Cu grids after being hydrophilized by glow discharge. The average diameters of the GNPs were determined from the TEM images by measuring *ca.* 500 particles using Image *J* software (version 1.45, National Institutes of Health, USA), and the surface areas of GNP particles were calculated from the obtained average diameters. The amount of carbohydrate conjugated to GNPs was quantified by elemental analysis after purification above mentioned, and the number of sugar chains existing on one GNP particle was calculated based on the molecular weight of βGlc***n*** (***n*** = 6; 990.89, ***n*** = 15; 2450.19).

2.4. Lectin assay

ConA-mediated aggregation behavior was monitored in the presence of βGlc***n***-GNPs to evaluate the βGlc***n***-GNP affinity for ConA in terms of surface sugar density. Glyco-conjugated GNPs were dispersed in deionized water, and the initial absorbance was adjusted to *ca.* 0.5 at *ca.* 520 nm. The designated glyco-conjugated GNP solution (0.2 mg mL^{-1}, 600 μL) was added to the ConA solution (128 nmol L^{-1}, 300 μL), and a half-value time—the time required to reach half absorbance—was determined. Reference lectins such as PNA that have no Glc-binding properties, and typical protein BSA, were measured in a similar manner as controls.

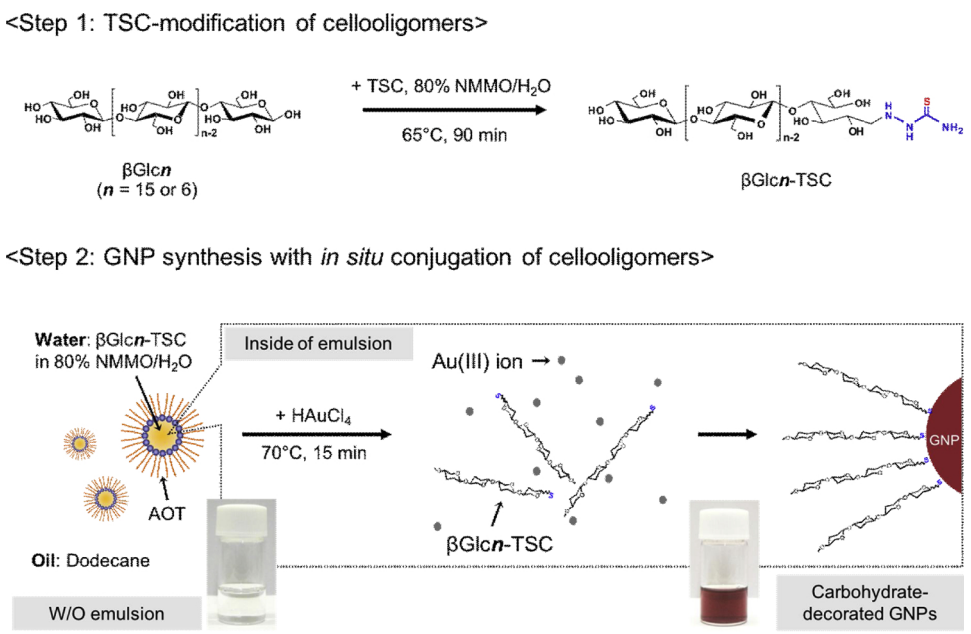

Fig. 1. Schematic illustration of the synthesis of carbohydrate-decorated gold nanoparticles (GNPs), and optical images before and after βGlc***n***-GNPs synthesis.

3. Results and discussion

3.1. Structural characterization of cellooligomer-conjugated GNPs

The NMMO-mediated GNP synthesis that was established in a previous report [29] was applied to a W/O emulsion system to fine-tune the nanosized morphology of glyco-conjugated GNPs. A dilute solution of $HAuCl_4$ was added dropwise to a W/O emulsion composed of βGlc***n*** containing-NMMO/water and dodecane stabilized by AOT, with stirring at 70 °C; and the mixed W/O emulsion immediately changed from colorless to a reddish-purple (Fig. 1). UV–vis absorption spectra of the W/O emulsion displayed clear SPR band at *ca.* 520 nm as shown in Fig. 2, and became sharper with an increase in the concentration of βGlc15-TSCs without any wavelength shift. In contrast, the NMMO/H_2O single phase system without dodecane or AOT exhibited broader SPR band at *ca.* 530 nm [29]. In general, the SPR absorbance behavior depends on the size and shape of GNPs, and shorter wavelengths suggest smaller GNPs [5]. The results revealed that NMMO-mediated GNP synthesis was possible in the W/O emulsion system and that the approach contributed to the narrow size distribution of the as-synthesized GNPs. In addition, the conjugation of βGlc***n***-TSCs resulted in a narrower size distribution for βGlc***n***-GNPs, than for GNPs, possibly due to the protection provided against GNP self-aggregation. As the βGlc***n***-TSC concentration increased, the surfaces of GNPs were further covered by the βGlc***n*** sugar chains, resulting in inhibition of GNP self-aggregation and increase in each absorbance in Fig. 2. There was little difference found in the UV–vis spectra of the W/O emulsions containing high concentrations of βGlc15-TSCs—4.0 and 8.0 mmol L^{-1}. Thus, these concentrations were regarded as limiting conditions.

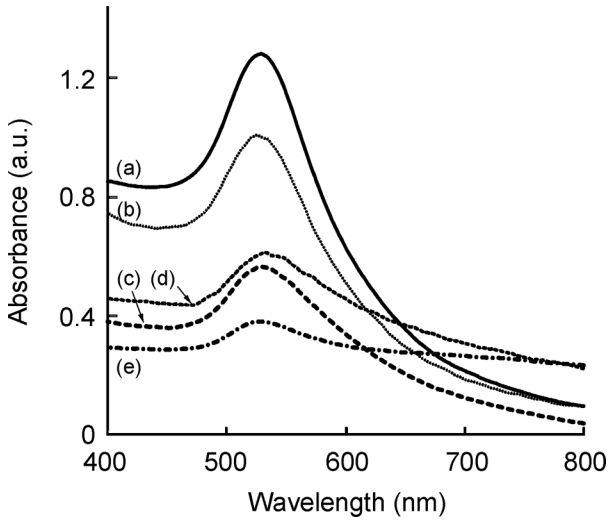

Fig. 2. UV–vis spectra of βGlc15-GNPs synthesized in a W/O emulsion system. βGlc15-TSC concentrations in the water phase were 8.0 mmol L^{-1} (a), 4.0 mmol L^{-1} (b), 2.0 mmol L^{-1} (c), 1.0 mmol L^{-1} (d), and 0.4 mmol L^{-1} (e).

As-synthesized GNPs and βGlc***n***-GNPs were thoroughly washed to remove NMMO, AOT and unreacted βGlc***n***-TSCs (see Experimental section). After freeze-drying, the purified GNPs and βGlc***n***-GNPs were used for further study. Table 1 lists the average diameters obtained from the TEM images (Figure S1) and the calculated coefficient of variation (CV) values of βGlc***n***-TSCs. In the absence of sugar-TSCs, clear GNP aggregation was observed due to unstable GNP surfaces (Figure S2). In contrast, the conjugation of βGlc***n***-TSCs led to clear dispersion of as-synthesized βGlc***n***-GNPs, while maintaining the size uniformity. Both size and distribution improved with increasing βGlc***n***-TSC concentration, suggesting that the conjugated sugars served as effective dispersants for GNPs. The βGlc15-GNPs had a uniform size distribution compared with the βGlc6-GNPs, possibly indicating that longer sugar chains were more effective for size control and dispersion. However, excess βGlc15-TSCs had a negative influence on the nanomorphology, possibly owing to partial precipitation of βGlc15-TSCs in the W/O emulsion system; hence in this study, 4.0 mmol L^{-1} was the most suitable concentration to give βGlc15-GNPs with small size and narrow size distribution. In the case of βGlc6-GNPs, a clear trend was not observed. In a previous study, we reported the first preparation of GNPs in hot 80% NMMO/20% H_2O solution using the auto-redox mechanism [29]; however the obtained sugar-conjugated GNPs were not uniform, exhibiting a large distribution of average sizes (6.8 ± 1.7 nm, CV = *ca.* 25% for βGlc15-GNPs, and 4.8 ± 1.4 nm, CV = *ca.* 29% for βGlc7-GNPs). In the batch reaction system using mL-scale NMMO solution, aurate ions were very rapidly reduced to form GNPs, presumably leading to uncontrolled crystal growth of GNPs. In contrast, the W/O emulsion system provided the limited volume of the micro-emulsion particles for reduction under mild controlled conditions; then the stable growth of GNPs and *in situ* surface modification with βGlc***n***-TSCs

Table 1
Characterization of βGlc***n***-GNPs.

Sample	βGlc***n*** concentration (mmol L^{-1})	Particle size (nm)	Coefficient of variation (%)	Surface sugar density (chains nm^{-2})	Time of half-absorbance (min)*
βGlc15-GNP-1	1.0	11.72 ± 2.13	18.2	0.033	20
βGlc15-GNP-2	2.0	11.62 ± 1.36	11.7	0.17	15
βGlc15-GNP-4	4.0	10.50 ± 0.74	7.05	0.51	5
βGlc15-GNP-8	8.0	11.39 ± 0.95	8.34	0.77	20
βGlc6-GNP-1	1.0	11.94 ± 3.57	29.9	0.012	60
βGlc6-GNP-2	2.0	11.92 ± 2.72	22.8	0.086	40
βGlc6-GNP-4	4.0	11.31 ± 2.10	18.6	0.21	30
βGlc6-GNP-8	8.0	11.67 ± 2.38	20.4	0.14	30

Carbohydrate-conjugated GNPs were synthesized with *S*-derivatized cellooligomers (βGlc15-TSC or βGlc6-TSC).
* Time of half-absorbance is the time required to reach half absorbance by adding 42.7 nmol L^{-1} of ConA.

occurred. Therefore, microreaction in a W/O emulsion system was effective for fine-tuning the nanomorphology of carbohydrate–GNP conjugates.

3.2. Regulation of surface sugar density on cellooligomers–GNP conjugates

The surface density of βGlc***n*** chains immobilized on a single GNP was determined from the results of elemental analysis of βGlc***n***-GNPs and the relative surface areas calculated from the average diameters of GNPs, estimated by TEM observation. The sugar densities of βGlc***n***-GNPs ranged from 0.012 to 0.77 chains nm^{-2}, depending on chain length and concentration in the synthesis (Table 1). It was revealed that the sugar concentrations in the preparations did not always correlate with the final amounts of carbohydrate on the GNP surfaces owing to different conjugation efficiencies in each case. We would therefore like to highlight potential problems in previous reports in which the actual sugar density on the GNP surfaces was not determined, and the concentrations of sugar used were regarded as being proportional to apparent sugar density [22,23]. In contrast, in this study actual sugar density was roughly determined using analytical techniques. The sugar density of βGlc***n***-GNPs increased with increases in the βGlc***n***-TSC concentration of the W/O emulsion; however, it was not a linear relationship, and plateau behavior was observed at high concentrations. Thus, the conjugation efficiency was presumed to be reduced by increasing molar ratios of carbohydrate-TSCs and gold species. Table 1 also shows that the βGlc15-GNPs had higher sugar densities than βGlc6-GNPs at all concentrations, even though shorter chains presumably have less steric hindrance. This is an interesting finding and could be attributed to the stronger intermolecular interaction of βGlc15 compared with water-soluble βGlc6, leading to a larger number of sugar chains being accumulated on the βGlc15-GNP surfaces.

The achieved sugar densities, 0.21 and 0.77 chains nm^{-2} for βGlc6-GNPs and βGlc15-GNPs, respectively, were relatively high compared with those obtained using a general grafting-to approach to accumulate long molecules on particle surfaces. The polymer chains must diffuse through the existing polymer layer to reach the reaction sites, therefore, only a small number of polymer chains can be immobilized on surfaces using the grafting-to method [31]. In contrast, structural oligosaccharides are thought to arrange with high density on GNP surfaces owing to molecular association *via* intermolecular hydrogen bonding, as previously reported for the hybrid interface of βGlc6 and βGlcNAc6 [32]. Longer chains (βGlc15) would be expected to exhibit strong interaction between chains to give a denser crowding arrangement than shorter chains (βGlc6). However, long-chain cellooligomers are soluble in neither water nor common organic solvents, and therefore it is generally difficult to immobilize them on GNP surfaces. In this study, our novel strategy enabled high-density functionalization with long-chain cellooligomers, through the one-step NMMO-mediated GNP synthesis and simultaneous *in situ* glyco-surface modification in the same NMMO/H_2O solvent. Hence, the specific self-assembly of cellulose was successfully applied to increase the surface sugar density; longer chains led to higher density. Self-assembly features based on the formation of regular intra- and inter-molecular hydrogen bonds are expected to make a potential contribution to the functional clustering of carbohydrates immobilized on GNP surfaces. Tailoring of βGlc***n***-GNPs with controlled sugar density was achieved using this facile technique, and in the following section the affinity of βGlc***n***-GNPs for ConA is discussed in relation to the surface sugar density.

3.3. Lectin response behavior for cellooligomer-clustered GNPs

The addition of ConA to the suspension of βGlc***n***-GNPs immediately caused a color change from red to purple and over time dark-purple aggregates precipitated at the bottom of the test tube, as shown in Fig. 3a. In addition, the self-assembly behavior depended on the concentration of ConA. In the case of Glc15-GNPs the half-value color change occurred in 5 and 30 min at final ConA concentrations of 42.7 and 5.3 nmol L^{-1}, respectively. ConA-mediation gave rise to broader spectra and the SPR band shifted to longer wavelength with time, possibly as a result of the aggregation of βGlc15-GNPs suspended in solution (Fig. 4a). ConA is a tetramer at physiological pH [33]. Each subunit has a single saccharide binding site that recognizes glucoside at

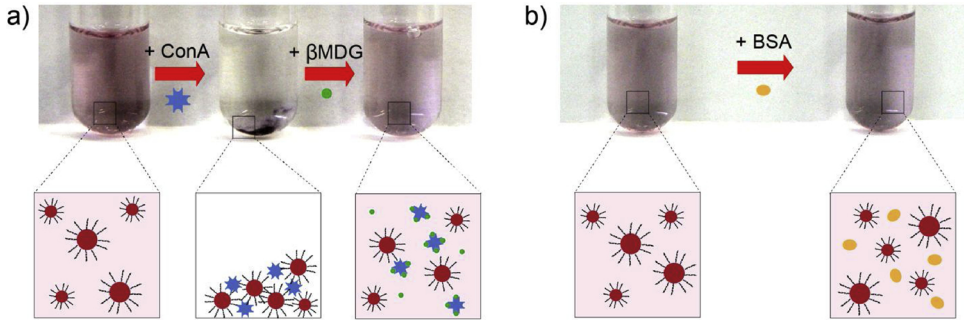

Fig. 3. Specific interaction between βGlc15-GNPs and concanavalin A (ConA). a) ConA was added to a βGlc15-GNPs suspension, resulting in rapid aggregation of ConA–βGlc15-GNPs. The aggregates were rapidly re-suspended by adding methyl-β-D-glucopyranoside (βMDG). b) BSA addition (no change in color).

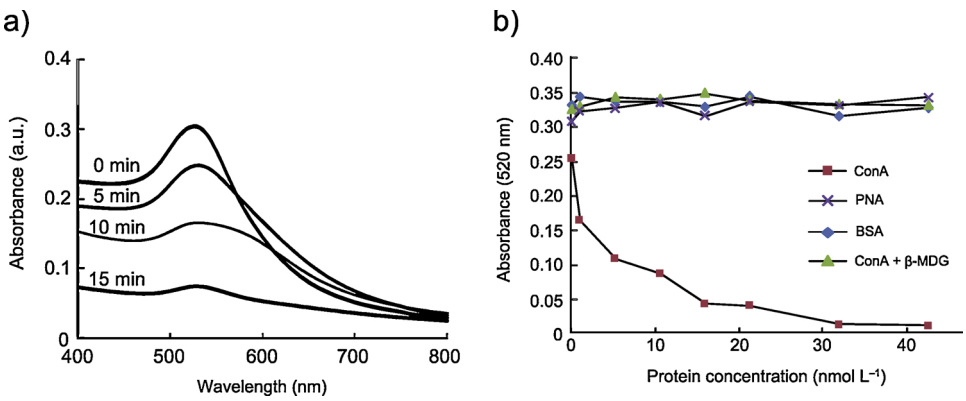

Fig. 4. Time- and concentration-dependent absorbance changes. a) Time-dependent spectral changes for βGlc15-GNP-4 suspension containing 1.1 nmol L^{-1} ConA. b) Concentration-dependent changes in the absorbance at 520 nm for βGlc15-GNP-4 suspensions of varying protein concentration. Each protein—ConA, peanut agglutinin (PNA), and bovine serum albumin (BSA)—was mixed with βGlc15-GNPs. The absorbance at 520 nm was measured after 10 min. Methyl-β-D-glucopyranoside (βMDG) was added as an inhibitor of ConA lectin binding to βGlc15-GNPs.

the non-reducing end of oligosaccharides [34], therefore ConA could crosslink with multiple βGlc15-GNPs *via* glyco-receptors (see schematic illustration in Fig. 3a). Native GNPs without βGlc15 showed no interaction with ConA (Fig. S3). Fig. 4b shows the absorbance changes of βGlc15-GNP-4 (amount of βGlc15-TSC; 4 mmol L^{-1}) 10 min after adding a variety of ConA, PNA, and BSA concentrations (0.11–42.7 nmol L^{-1}). The absorbance of βGlc15-GNP-4 with ConA gradually decreased as the ConA concentration increased. Neither PNA, which exhibits specific recognition for D-Gal, nor typical protein BSA, showed significant interactions with βGlc15-GNP-4 (Figs. 3b and 4b). As-formed ConA–βGlc15-GNP-4 complex was immediately eliminated by adding methyl β-D-glucopyranoside (βMDG) solution (2 μmol L^{-1}), as shown in Fig. 3a; the color of the suspension immediately recovered the original red through the re-dispersion of βGlc15-GNPs detached from ConA. Therefore, ConA specifically interacted with the non-reducing ends of βGlc15 conjugated to the GNP surfaces, and reversibly dissociated from βGlc15-GNPs in the presence of large amounts of free carbohydrates such as βMDG. These dispersion and aggregation cycles could be repeated through the addition of ConA and free βMDG. In addition, the βGlc***n***-GNPs were easily recovered by centrifugation after sonication, and could thus be used as a biosensor.

A clear relationship between sugar density and lectin-binding affinity is shown in Table 1. Cellooligomer-clustered GNPs had unique characteristics of ConA affinity. In the case of βGlc15-GNPs, the apparent affinity increased with increasing surface sugar density, however excess amounts of βGlc15 on the GNP surfaces reduced their affinity for ConA. It is suggested that the lectin affinity is closely related to the surface sugar density, and in this study a density of 0.51 chains nm^{-2} was found to be optimal for the interactive response to ConA. In this case, apparent detection limit might be considered around 1.1 nmol L^{-1} for ConA. The ConA used in this work has four binding sites, which are located in the distance of *ca.* 6.5 nm [35]. Therefore, an appropriate distance of βGlc***n*** on the GNP surface was assumed for optimal interaction with ConA. Longer chain βGlc15-GNPs showed higher interaction with ConA in all cases. The highest density of βGlc6-GNPs was almost the same as the lowest density of βGlc15-GNPs, however the affinity of βGlc15-GNPs for ConA was stronger than that of βGlc6-GNPs. This result suggests that the longer chains were preferably recognized by ConA owing to the fluctuation of the non-reducing ends compared with those of the shorter chains with less steric hindrance. Our synthesized βGlc15-GNPs demonstrated a high affinity and sensitive response to ConA, possibly as a result of β-D-Glc clustering on the GNP surfaces. Tailoring the carbohydrate moieties conjugated to GNPs would provide novel nanomaterials for the efficient detection of various biomolecules and is expected to have applications in cell assays using visual detection.

4. Conclusion

We successfully synthesized novel carbohydrate-conjugated GNPs in a W/O emulsion system *via* NMMO-mediated GNP synthesis and simultaneous *in situ* conjugation of cellooligomers to the GNP surfaces. Monodisperse carbohydrate-GNP conjugates were prepared in a one-pot, one-step reaction. Molecular association of cellulose *via* intermolecular hydrogen bonding led to a high density of βGlc***n*** moieties on the GNPs surfaces. The sugar density was controllable, and closely related to the interaction with ConA. The high sensitivity response to ConA aggregation was thought to be induced by the cluster glycoside effect of as-designed glyco-GNPs. The lectin binding to glyco-ligands on the GNPs was profoundly affected by how the ligands were displayed on the GNP surface. This finding is of great significance for tuning functional sugar-conjugated GNPs. The simple approach for preparation of carbohydrate-decorated GNPs could open up significant opportunities for glyco-nanomaterials engineering.

Acknowledgments

This research was supported by Grants-in-Aid for Scientific Research (B: 26292096 and A: 17H01482) from the Ministry of Education, Culture, Sports, Science and Technology of Japan (T.K.).

Appendix A. Supplementary data

Supplementary material related to this article can be found, in the online version, at doi:https://doi.org/10.1016/j.colsurfb.2019.02.051.

References

[1] T.K. Sau, A.L. Rogach, F. Jäckel, T.A. Klar, J. Feldmann, Properties and applications of colloidal nonspherical noble metal nanoparticles, Adv. Mater. 22 (2010) 1805–1825, https://doi.org/10.1002/adma.200902557.
[2] M. Hu, J. Chen, Z.-Y. Li, L. Au, G.V. Hartland, X. Li, M. Marquez, Y. Xia, Gold nanostructures: engineering their plasmonic properties for biomedical applications, Chem. Soc. Rev. 35 (2006) 1084–1094, https://doi.org/10.1039/B517615H.
[3] C.K. Adokoh, S. Quan, M. Hitt, J. Darkwa, P. Kumar, R. Narain, Synthesis and evaluation of glycopolymeric decorated gold nanoparticles functionalized with gold-triphenyl phosphine as anti-cancer agents, Biomacromolecules 15 (2014) 3802–3810, https://doi.org/10.1021/bm5010977.
[4] A. Lemelle, B. Veksler, I.S. Kozhevnikov, G.G. Akchurin, S.A. Piletsky, I. Meglinski, Application of gold nanoparticles as contrast agents in confocal laser scanning microscopy, Laser Phys. Lett. 6 (2009) 71–75 http://stacks.iop.org/1612-202X/6/i=1/a=013.
[5] S. Link, M.A. El-Sayed, Size and temperature dependence of the plasmon absorption of colloidal gold nanoparticles, J. Phys. Chem. B 103 (1999) 4212–4217, https://doi.org/10.1021/jp984796o.
[6] S. Eustis, M.A. El-Sayed, Why gold nanoparticles are more precious than pretty gold: Noble metal surface plasmon resonance and its enhancement of the radiative and nonradiative properties of nanocrystals of different shapes, Chem. Soc. Rev. 35 (2006) 209–217, https://doi.org/10.1039/B514191E.
[7] K.H. Su, Q.H. Wei, X. Zhang, J.J. Mock, D.R. Smith, S. Schultz, Interparticle coupling effects on Plasmon resonances of nanogold particles, Nano Lett. 3 (2003) 1087–1090, https://doi.org/10.1021/nl034197f.
[8] M. Brust, M. Walker, D. Bethell, D.J. Schiffrin, R. Whyman, Synthesis of thiol-derivatised gold nanoparticles in a two-phase liquid–liquid system, J. Chem. Soc. Chem. Commun. (1994) 801–802, https://doi.org/10.1039/C39940000801.
[9] D.V. Leff, L. Brandt, J.R. Heath, Synthesis and characterization of hydrophobic,

organically-soluble gold nanocrystals functionalized with primary amines, Langmuir 12 (1996) 4723–4730, https://doi.org/10.1021/la960445u.
[10] M.A. Aziz, J.P. Kim, M. Oyama, Preparation of monodispersed carboxylate-functionalized gold nanoparticles using pamoic acid as a reducing and capping reagent, Gold Bull. 47 (2014) 127–132, https://doi.org/10.1007/s13404-014-0134-0.
[11] J.M. de la Fuente, A.G. Barrientos, T.C. Rojas, J. Rojo, J. Cañada, A. Fernández, S. Penadés, Gold glyconanoparticles as water-soluble polyvalent models to study carbohydrate interactions, Angew. Chemie Int. Ed. 40 (2001) 2257–2261, https://doi.org/10.1002/1521-3773(20010618)40:12<2257 AID-ANIE2257 > 3.0. CO;2-S.
[12] Y. Ding, Z. Jiang, K. Saha, C.S. Kim, S.T. Kim, R.F. Landis, V.M. Rotello, Gold nanoparticles for nucleic acid delivery, Mol. Ther. 22 (2014) 1075–1083 doi:1038/mt.2014.30.
[13] N.G. Bastús, E. Sánchez-Tilló, S. Pujals, C. Farrera, C. López, E. Giralt, A. Celada, J. Lloberas, V. Puntes, Homogeneous conjugation of peptides onto gold nanoparticles enhances macrophage response, ACS Nano 3 (2009) 1335–1344, https://doi.org/10.1021/nn8008273.
[14] C.J. Thibodeaux, C.E. Melançon, H. Liu, Unusual sugar biosynthesis and natural product glycodiversification, Nature 446 (2007) 1008, https://doi.org/10.1038/nature05814.
[15] A. Varki, Glycan-based interactions involving vertebrate sialic-acid-recognizing proteins, Nature 446 (2007) 1023, https://doi.org/10.1038/nature05816.
[16] F.A. Quiocho, Protein-carbohydrate interactions: basic molecular features, Pure Appl. Chem. 61 (1989) 1293–1306, https://doi.org/10.1351/pac198961071293.
[17] S. Suvarna, U. Das, S. Kc, S. Mishra, M. Sudarshan, K. Das Saha, S. Dey, A. Chakraborty, Y. Narayana, Synthesis of a novel glucose capped gold nanoparticle as a better theranostic candidate, PLoS One 12 (2017) e0178202, , https://doi.org/10.1371/journal.pone.0178202.
[18] B. Arnáiz, O. Martínez-Ávila, J.M. Falcon-Perez, S. Penadés, Cellular uptake of gold nanoparticles bearing HIV gp120 oligomannosides, Bioconjug. Chem. 23 (2012) 814–825, https://doi.org/10.1021/bc200663r.
[19] C. Zhu, Q. Zheng, L. Wang, H.F. Xu, J. Tong, Q. Zhang, Y. Wan, J. Wu, Synthesis of novel galactose functionalized gold nanoparticles and its radiosensitizing mechanism, J. Nanobiotechnology 13 (2015) 67, https://doi.org/10.1186/s12951-015-0129-x.
[20] F.W. Shen, K.C. Zhou, H. Cai, Y.N. Zhang, Y.L. Zheng, J. Quan, One-pot synthesis of thermosensitive glycopolymers grafted gold nanoparticles and their lectin recognition, Colloids Surf. B Biointerfaces 173 (2019) 504–511, https://doi.org/10.1016/j.colsurfb.2018.10.028.
[21] X. Jiang, A. Housni, G. Gody, P. Boullanger, M.T. Charreyre, T. Delair, R. Narain, Synthesis of biotinylated α-d-mannoside or N-acetyl β-d-glucosaminoside decorated gold nanoparticles: study of their biomolecular recognition with Con A and WGA lectins, Bioconjug. Chem. 21 (2010) 521–530, https://doi.org/10.1021/bc900431p.
[22] H. Uzawa, K. Ohga, Y. Shinozaki, I. Ohsawa, T. Nagatsuka, Y. Seto, Y. Nishida, A novel sugar-probe biosensor for the deadly plant proteinous toxin, ricin, Biosens. Bioelectron. 24 (2008) 923–927, https://doi.org/10.1016/j.bios.2008.07.049.
[23] D.C. Hone, A.H. Haines, D.A. Russell, Rapid, quantitative colorimetric detection of a lectin using mannose-stabilized gold nanoparticles, Langmuir 19 (2003) 7141–7144, https://doi.org/10.1021/la034358v.
[24] Y.C. Lee, R.T. Lee, Carbohydrate-protein interactions: basis of glycobiology, Acc. Chem. Res. 28 (1995) 321–327, https://doi.org/10.1021/ar00056a001.
[25] J.J. Lundquist, E.J. Toone, The cluster glycoside effect, Chem. Rev. 102 (2002) 555–578, https://doi.org/10.1021/cr000418f.
[26] Y.Y. Chien, M.D. Jan, A.K. Adak, H.C. Tzeng, Y.P. Lin, Y.J. Chen, K.T. Wang, C.T. Chen, C.C. Chen, C.C. Lin, Globotriose-functionalized gold nanoparticles as multivalent probes for shiga-like toxin, ChemBioChem 9 (2008) 1100–1109, https://doi.org/10.1002/cbic.200700590.
[27] D. Klemm, B. Heublein, H.P. Fink, A. Bohn, Cellulose: fascinating biopolymer and sustainable raw material, Angew. Chemie Int. Ed. 44 (2005) 3358–3393, https://doi.org/10.1002/anie.200460587.
[28] M. Umemura, Y. Yuguchi, T. Hirotsu, Interaction between cellooligosaccharides in aqueous solution from molecular dynamics simulation: comparison of cellotetraose, cellopentaose, and cellohexaose, J. Phys. Chem. A 108 (2004) 7063–7070, https://doi.org/10.1021/jp049044a.
[29] S. Yokota, T. Kitaoka, M. Opietnik, T. Rosenau, H. Wariishi, Synthesis of gold nanoparticles for in situ conjugation with structural carbohydrates, Angew. Chemie Int. Ed. 47 (2008) 9866–9869, https://doi.org/10.1002/anie.200803922.
[30] A. Isogai, M. Usuda, Preparation of low-molecular weight celluloses using phosphoric acid, Mokuzai Gakkaishi 37 (1991) 339–344.
[31] B. Zdyrko, I. Luzinov, Polymer brushes by the “grafting to” method, Macromol. Rapid Commun. 32 (2011) 859–869, https://doi.org/10.1002/marc.201100162.
[32] Y. Yoshiike, T. Kitaoka, Tailoring hybrid glyco-nanolayers composed of chitohexaose and cellohexaose for cell culture applications, J. Mater. Chem. 21 (2011) 11150–11158, https://doi.org/10.1039/C1JM11448D.
[33] J.L. Wang, G.M. Edelman, Binding and functional properties of concanavalin A and its derivatives. II. A proteolytic product with saccharide-binding activity, J. Biol. Chem. 253 (1978) 3008–3015, http://www.jbc.org/content/253/9/3008.abstract.
[34] I.J. Goldstein, C.E. Hollerman, J.M. Merrick, Protein-carbohydrate interaction I. The interaction of polysaccharides with concanavalin A, Biochim. Biophys. Acta 97 (1965) 68–76, https://doi.org/10.1016/0304-4165(65)90270-9.
[35] B.M. Cummins, J.T. Garza, G.L. Coté, Optimization of a Concanavalin A-based glucose sensor using fluorescence anisotropy, Anal. Chem. 85 (2013) 5397–5404, https://doi.org/10.1021/ac303689j.